

Thermal convection for large Prandtl numbers

Siegfried Grossmann¹ and Detlef Lohse²

¹ *Department of Physics, University of Marburg, Renthof 6, D-35032 Marburg, Germany*

² *Department of Applied Physics and J. M. Burgers Centre for Fluid Dynamics, University of Twente, 7500 AE Enschede, Netherlands*

(October 27, 2018)

The Rayleigh-Benard theory by Grossmann and Lohse [J. Fluid Mech. 407, 27 (2000)] is extended towards very large Prandtl numbers Pr . The Nusselt number Nu is found here to be independent of Pr . However, for fixed Rayleigh numbers $Ra > 10^{10}$ a maximum around $Pr \approx 2$ in the $Nu(Pr)$ -dependence is predicted which is absent for lower Ra . We moreover offer the full functional dependences of $Nu(Ra, Pr)$ and $Re(Ra, Pr)$ within this extended theory, rather than only giving the limiting power laws as done in ref. [1]. This enables us to more realistically describe the *transitions* between the various scaling regimes, including their widths.

In thermal convection, the control parameters are the Rayleigh number Ra and the Prandtl number Pr . The system responds with the Nusselt number Nu (the dimensionless heat flux) and the Reynolds number Re (the dimensionless large scale velocity). The key question is to understand the dependences $Nu(Ra, Pr)$ and $Re(Ra, Pr)$. In experiments, traditionally the Prandtl number was more or less kept fixed [2–4]. However, the recent experiments in the vicinity of the critical point of helium gas [5, 6] and of SF₆ [7] or with various alcohols [8] allow to vary both Ra and Pr and thus to explore a larger domain of the $Ra-Pr$ parameter space of Rayleigh-Benard (RB) convection, in particular that for $Pr \gg 1$. While the experiments of Steinberg’s group [7] suggest a decreasing Nusselt number with increasing Pr , namely $Nu = 0.22Ra^{0.3 \pm 0.03} Pr^{-0.2 \pm 0.04}$ in $10^9 \leq Ra \leq 10^{14}$ and $1 \leq Pr \leq 93$, the experiments of the Ahlers group suggest a saturation of Nu with increasing Pr for fixed Ra , at least up to $Ra = 10^{10}$ [9]. The same saturation (at fixed $Ra = 6 \cdot 10^5$) is found in the numerical simulations by Verzicco and Camussi [10] and Herring and Kerr [11].

The large Pr regime of the latest experiments has not been covered by the recent theory on thermal convection by Grossmann and Lohse (GL, [1]), which otherwise does pretty well in accounting for various measurements. In particular, it explains the low Pr measurements of Cioni et al. [4] ($Pr = 0.025$), the low Pr numerics which reveal $Nu \sim Pr^{0.14}$ for fixed Ra [10, 11], and the above mentioned experiments by Niemela et al. [6] and Xu et al. [8].

In the present paper we extend the GL theory in a natural way to the regime of very large Pr , on which no statement has been made in the original paper [1]. We find Nu to be independent of Pr in that regime. We in addition present the complete functional dependences $Nu(Ra, Pr)$ and $Re(Ra, Pr)$ within the GL theory, rather than only giving the limiting power laws and superpositions of those as was done in [1]. This enables us to more realistically describe the *transitions* between the various scaling regimes found already in [1].

Approach: To make this paper selfcontained we very briefly recapitulate the key idea of the GL theory, which is to decompose in the volume averages of the energy dissipation rate ϵ_u and the thermal dissipation rate ϵ_θ into their boundary layer (BL) and bulk contributions,

$$\epsilon_u = \epsilon_{u,BL} + \epsilon_{u,bulk}, \quad (1)$$

$$\epsilon_\theta = \epsilon_{\theta,BL} + \epsilon_{\theta,bulk}. \quad (2)$$

For the left hand sides the exact relations $\epsilon_u = \frac{\nu^3}{L^4}(Nu - 1)RaPr^{-2}$ and $\epsilon_\theta = \kappa \frac{\Delta^2}{L^2}Nu$ are used, where ν is the kinematic viscosity, κ the thermal diffusivity, L the height of the cell, and Δ the temperature difference between the bottom and the top plates. Next, the local dissipation rates in the BL and in the bulk (right hand sides of eqs. (1) and (2)) are modelled as the corresponding energy input rates, i.e., in terms of U , Δ , and the widths λ_u and λ_θ of the kinetic and thermal boundary layers, respectively. For the thickness of the thermal BL we assume $\lambda_\theta = L/(2Nu)$ and for that of the kinetic one $\lambda_u = L/(4\sqrt{Re})$ as it holds in Blasius type layers [12]; as for the prefactor 1/4 cf. [1], Sec. 4.3. For very large Ra the laminar BL will become turbulent and λ_u will show a stronger Re dependence. Note that whereas the thermal BLs only build up at the top and bottom wall, the kinetic BL occurs at *all* walls of the cell and therefore the contribution of $\epsilon_{u,BL}$ to ϵ_u is larger than a simple minded argument would suggest. The two eqs. (1) and (2) then allow to calculate the two dependent variables Nu and Re as functions of the two independent ones Ra and Pr .

Input rate modeling: The modeling of the dissipation rates on the rhs of eqs. (1) and (2) is guided by the Boussinesq equations. Depending on whether the BL or the bulk contributions are dominant, one gets different expressions on the rhs of eqs. (1), (2) and thus different relations for Nu , Re vs. Ra , Pr , defining different main regimes, see ref. [1] and fig. 1.

The rhs thermal dissipation rates depend on whether the kinetic BL of thickness λ_u is within the thermal BL of thickness λ_θ ($\lambda_u < \lambda_\theta$, small Pr) or vice versa ($\lambda_u > \lambda_\theta$, large Pr). The line $\lambda_u = \lambda_\theta$, corresponding to $Nu = 2\sqrt{Re}$, splits the phase diagram into a lower (small Pr) and an upper (large Pr) part, which we shall label by “ ℓ ” and “ u ”.

We first consider $\lambda_u < \lambda_\theta$ (i.e., small Pr , regime “ ℓ ”). Then (see [1])

$$\epsilon_{u,bulk} \sim \frac{U^3}{L} \sim \frac{\nu^3}{L^4}Re^3, \quad (3)$$

$$\epsilon_{u,BL} \sim \nu \frac{U^2 \lambda_u}{\lambda_u^2 L} \sim \frac{\nu^3}{L^4}Re^{5/2}, \quad (4)$$

$$\epsilon_{\theta,bulk} \sim \frac{U\Delta^2}{L} \sim \kappa \frac{\Delta^2}{L^2}PrRe, \quad (5)$$

$$\epsilon_{\theta,BL} \sim \kappa \frac{\Delta^2}{L^2}(RePr)^{1/2}. \quad (6)$$

The last expression is concluded [1, 3, 13] from the heat transfer equation $u_x \partial_x \theta + u_z \partial_z \theta = \kappa \partial_z^2 \theta$, which implies $U/L \sim \kappa/\lambda_\theta^2$ giving $Re^{1/2}Pr^{1/2} \sim Nu$.

If now larger Pr are considered, the kinetic boundary will eventually exceed the thermal one, $\lambda_u > \lambda_\theta$, upper range “ u ”. The relevant velocity at the edge between the thermal BL and the thermal bulk now is less than U , about $U\lambda_\theta/\lambda_u$. To describe the transition from λ_u being smaller to being larger than λ_θ we introduce the function $f(x) = (1 + x^n)^{-1/n}$ of the variable $x_\theta = \lambda_u/\lambda_\theta = c_\theta Nu/2\sqrt{Re}$, f being 1 in the lower range “ ℓ ” (small Pr) and $1/x_\theta$

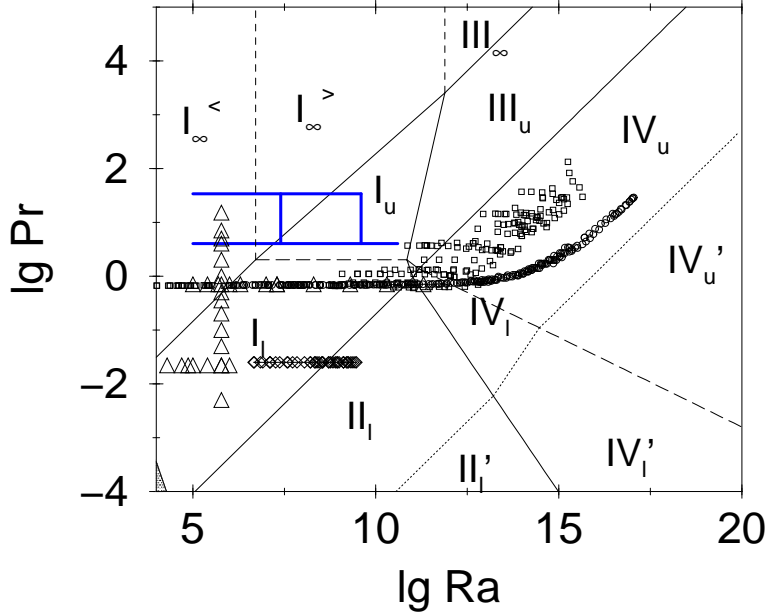


FIG. 1. Phase diagram in the $Ra - Pr$ plane, with data points included where Nu has been measured or numerically calculated. Squares show measuring points of Chavanne et al. [5], diamonds those by Cioni et al. [4], circles those by Niemela et al. [6], the very thick lines those by Xu et al. [8], and the triangles are those points for which Verzicco and Camussi did full numerical simulations [10]. The long-dashed line is the line $\lambda_u = \lambda_\theta$. The thin dotted line denotes where the laminar kinetic BL becomes turbulent. As extensively discussed in ref. [1], the exact onset of this instability strongly depends on the prefactors used when calculating this type of phase diagram. For this phase diagram the same prefactors as in ref. [1] have been chosen.

in “ u ” (large Pr), respectively. c_θ is about 1. The relevant velocity then is $Uf(x_\theta)$. We take $n = 4$ to characterize the sharpness of the transition.

This generalizes (5), (6) to

$$\epsilon_{\theta,bulk} \sim \kappa \frac{\Delta^2}{L^2} Pr Re f(c_\theta Nu / 2\sqrt{Re}), \quad (7)$$

$$\epsilon_{\theta,BL} \sim \kappa \frac{\Delta^2}{L^2} \sqrt{Pr Re f(c_\theta Nu / 2\sqrt{Re})}, \quad (8)$$

while $\epsilon_{u,bulk}$ and $\epsilon_{u,BL}$ are still given by (3),(4). Introducing (7),(8),(3),(4) into (1),(2) leads to the Ra, Pr dependences of Nu, Re in the upper regime “ u ”. The pure power laws $Nu(Ra, Pr)$ and $Re(Ra, Pr)$ in both the *lower* “ ℓ ” ($\lambda_u < \lambda_\theta$, small Pr) and the *upper* “ u ” ($\lambda_u > \lambda_\theta$, large Pr) regimes are summarized in table I.

Very large Pr regime: We now extend the theory to very large Prandtl numbers. As long as $Ra > Ra_c = 1708$ there still is wind, even for very large Pr , as Ra_c is independent of Pr . However, to keep Ra fixed, one has to increase the temperature difference Δ with

regime	dominance of	BLs	Nu	Re
I_l	$\epsilon_{u,BL}, \epsilon_{\theta,BL}$	$\lambda_u < \lambda_\theta$	$Ra^{1/4} Pr^{1/8}$	$Ra^{1/2} Pr^{-3/4}$
I_u		$\lambda_u > \lambda_\theta$	$Ra^{1/4} Pr^{-1/12}$	$Ra^{1/2} Pr^{-5/6}$
$I_\infty^<$		$\lambda_u = L/4 > \lambda_\theta$	$Ra^{1/3}$	$Ra^{2/3} Pr^{-1}$
$I_\infty^>$		$\lambda_u = L/4 > \lambda_\theta$	$Ra^{1/5}$	$Ra^{3/5} Pr^{-1}$
II_l	$\epsilon_{u,bulk}, \epsilon_{\theta,BL}$	$\lambda_u < \lambda_\theta$	$Ra^{1/5} Pr^{1/5}$	$Ra^{2/5} Pr^{-3/5}$
III_u	$\epsilon_{u,BL}, \epsilon_{\theta,bulk}$	$\lambda_u > \lambda_\theta$	$Ra^{3/7} Pr^{-1/7}$	$Ra^{4/7} Pr^{-6/7}$
III_∞		$\lambda_u = L/4 > \lambda_\theta$	$Ra^{1/3}$	$Ra^{2/3} Pr^{-1}$
IV_l	$\epsilon_{u,bulk}, \epsilon_{\theta,bulk}$	$\lambda_u < \lambda_\theta$	$Ra^{1/2} Pr^{1/2}$	$Ra^{1/2} Pr^{-1/2}$
IV_u		$\lambda_u > \lambda_\theta$	$Ra^{1/3}$	$Ra^{4/9} Pr^{-2/3}$

TABLE I. The power laws for Nu and Re of the presented theory. The regimes II_u and III_l are not included as they do not or hardly exist for the choice of prefactors.

increasing ν or Pr . $Pr \gg 1$ will lead to a smaller and smaller large scale wind Re . The flow will eventually become laminar throughout the cell. λ_u can no longer continue to increase according to $\lambda_u \sim Re^{-1/2}$ with decreasing Re , but will saturate to a constant value of order L . This is the central new point of the very large Pr regime. In [1] we had assumed that this happens at about $Re = 50$. This corresponds to a saturation at $\lambda_u = L/4\sqrt{Re} = L/28$. To model the smooth transition to the very large Pr regime beyond the line $Re = 50$, i.e., if $\lambda_u = L/4\sqrt{Re}$ approaches $\lambda_u = L/28$ we use the crossover function $g(x) = x(1 + x^n)^{-1/n}$ of the crossover variable $x_L = 28\lambda_u/L = 7/\sqrt{Re}$, and again $n = 4$. The function g increases linearly, $g(x_L) = x_L$, below the transition (x_L small) and is 1 in the very large Pr regime with $Re \leq 50$. In the above modelings for the local dissipation rates we have to replace each λ_u by $g(x_L)L/28$.

The resulting formulae, given momentarily, will lead, depending on Ra , to three new regimes, valid for very large Pr , denoted as $I_\infty^<$, $I_\infty^>$, and III_∞ , see Fig. 1 and Table I.

While eq. (3) for $\epsilon_{u,bulk}$ is assumed to still hold in the very large Pr range (where $\epsilon_{u,bulk}$ of course hardly contributes to ϵ_u due to the large extension of the kinetic BLs), eqs. (4), (5), and (6) have to be generalized. First generalize (4) for $\epsilon_{u,BL}$,

$$\epsilon_{u,BL} \sim \nu \frac{U^2}{g(x_L)L^2} \sim \frac{\nu^3}{L^4} \frac{Re^2}{g(7/\sqrt{Re})}. \quad (9)$$

Next $\epsilon_{\theta,bulk}$: Above the wind velocity U in (5), which sets the time scale of the stirring, has already been generalized to $Uf(\lambda_u/\lambda_\theta)$. This equals U itself in “ ℓ ” and $U\lambda_\theta/\lambda_u$ in the “ u ” regimes. Now in addition the explicit λ_u is to be replaced by $g(x_L)L/28$, i.e.,

$$\epsilon_{\theta,bulk} \sim \kappa \frac{\Delta^2}{L^2} Pr Re f\left(\frac{Nu}{14} g\left(\frac{7}{\sqrt{Re}}\right)\right). \quad (10)$$

This simplifies for large enough Ra (therefore large f -argument) and very large Pr (thus large g -argument) to

$$\epsilon_{\theta,bulk} \sim \kappa \frac{\Delta^2}{L^2} \frac{Pr Re}{Nu}. \quad (11)$$

Inserting (9) and (11) into the rhs of (1) and (2) leads to the new power laws describing the heat flux and the wind velocity in the regime III_∞ beyond III_u , cf. Figure 1,

$$Nu \sim Ra^{1/3} Pr^0, \quad Re \sim Ra^{2/3} Pr^{-1}. \quad (12)$$

Finally $\epsilon_{\theta,BL}$: In the thermal boundary layer range beyond I_ℓ , relevant for medium Ra , eq.(6) stays valid, because its derivation did not involve λ_u and also $f = 1$. The range $I_\infty^<$ has to be described by eqs.(1),(2),(9) (with $g = 1$), and (6), resulting in the same power laws as in regime III_∞ , i.e., eqs. (12). For Pr values above regime I_u eq.(6) no longer holds. It originated from the heat transport equation. There we have to use now $Uf(x_\theta)$ instead of merely U . The balance from the heat transfer equation then reads $Uf(x_\theta)/L \sim \kappa/\lambda_\theta^2$. In the f -argument $x_\theta = \lambda_u/\lambda_\theta$ the kinetic BL width λ_u and therefore the crossover function g appears, leading to

$$Pr Re f \left(\frac{Nu}{14} g \left(\frac{7}{\sqrt{Re}} \right) \right) \sim Nu^2. \quad (13)$$

In the very large Pr regime (where $g(x_L) = 1$) above I_u (where $f(x_\theta) = x_\theta^{-1}$) one obtains from (13) the relation $(RePr)^{1/3} \sim Nu$, valid in $I_\infty^>$. Together with (1), (2), and (9) one derives the new scaling laws in the interior of $I_\infty^>$

$$Nu \sim Ra^{1/5} Pr^0, \quad Re \sim Ra^{3/5} Pr^{-1}. \quad (14)$$

The scaling behavior $Nu \sim Ra^{1/5}$ has earlier been suggested by Roberts [14]. Note that in all three very large Pr regimes Nu does not depend on Pr . Furthermore the Constantin-Doering [15] upper bound $Nu \leq const Ra^{1/3} (1 + \log Ra)^{2/3}$, holding in the limit $Pr \rightarrow \infty$, is strictly fulfilled.

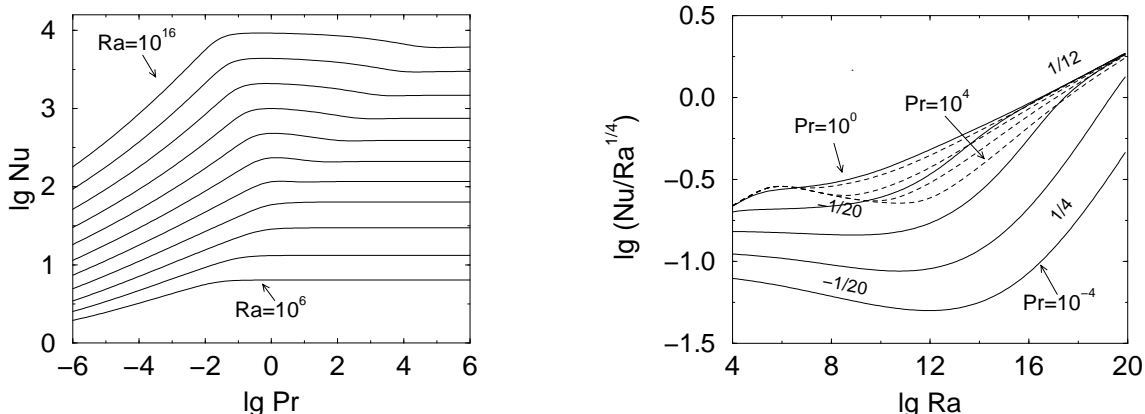


FIG. 2. (a) Nu as a function of Pr according to theory for $Ra = 10^6, Ra = 10^7, \dots$ to $Ra = 10^{16}$, bottom to top. (b) $Nu/Ra^{1/4}$ as function of Ra for $Pr = 10^{-4}, Pr = 10^{-3}, Pr = 10^{-2}, Pr = 10^{-1},$ and $Pr = 10^0$ (solid lines, bottom to top) and for $Pr = 10^1, Pr = 10^2, Pr = 10^3,$ and $Pr = 10^4$ (dashed lines, top to bottom).

Nu and Re in the whole parameter plane: Plugging now the general expressions for the local dissipation rates (3), (9), (10), and (13) into the balance eqs. (1) and (2) finally results in

$$NuRaPr^{-2} = c_1 \frac{Re^2}{g(7/\sqrt{Re})} + c_2 Re^3, \quad (15)$$

$$Nu = c_3 Re^{1/2} Pr^{1/2} \left[f \left(c_\theta \frac{Nu}{14} g \left(\frac{7}{\sqrt{Re}} \right) \right) \right]^{1/2} + c_4 Pr Re f \left(c_\theta \frac{Nu}{14} g \left(\frac{7}{\sqrt{Re}} \right) \right). \quad (16)$$

Here we have added dimensionless prefactors where appropriate to complete the modeling of the dissipation rates. In ref. [1] c_1 through c_5 were already adopted to Chavanne et al.'s experimental data [5]. The result was $c_1 = 1028$, $c_2 = 9.38$, $c_3 = 1.42$, $c_4 = 0.0123$, $1/c_\theta = c_5 = 2.0$, see eqs. (4.4) through (4.9) of [1]. Note that the c_i may depend on the aspect ratio and are not universal.

The set of eqs.(15) and (16) is the second main result of this paper. It allows to calculate $Nu(Ra, Pr)$ and $Re(Ra, Pr)$ in the whole $Ra - Pr$ parameter space, including all crossovers from any regime to any neighboring one. Technically, eq. (15) is solved for $Nu(Ra, Re, Pr)$ which then is inserted into eq. (16), leading to *one* implicit equation for $Re(Ra, Pr)$.

All limiting, pure scaling regimes which can be derived from eqs. (15) and (16) are listed in table I which extends table II of ref. [1], now including the three new regimes $I_\infty^<$, $I_\infty^>$, and III_∞ . The corresponding phase diagram is shown in figure 1, completing that of [1] towards very large Pr .

Though in the phase diagram we have drawn lines to indicate transitions between the regimes, defined by either $\epsilon_{u,BL} = \epsilon_{u,bulk}$ or $\epsilon_{\theta,BL} = \epsilon_{\theta,bulk}$ or $\lambda_u = \lambda_\theta$ or $\lambda_u = L/28$, we note that the crossovers are nothing at all but sharp. All transitions are smeared out over broad ranges, the more, the more similar the scaling exponents of the neighboring regimes are.

Discussion of $Nu(Pr)$ and $Nu(Ra)$: The functions $Nu(Pr)$ (for fixed values of Ra) and $Nu(Ra)/Ra^{1/4}$ (for fixed values of Pr) resulting from eqs. (15) - (16) are shown in figure 2. Indeed, for $Ra \approx 10^6 - 10^9$ the Nusselt number saturates with increasing Pr and the regime I_u with $Nu \sim Pr^{-1/12}$ is suppressed, in full agreement with the experimental and numerical results [9–11]. However, for larger Ra beyond $\approx 10^{11}$ the theory predicts a maximum for the curve $Nu(Pr)$. The decreasing branches of the curve for $Ra \approx 10^{12}$ and $Pr \approx 50$ may be consistent with above mentioned experimental results by Ashkenazi and Steinberg [7]. This observation may resolve the apparent discrepancy between the Ahlers et al. and the Steinberg et al. data: Simply different regimes in the $Ra - Pr$ phase space are probed.

The importance of transition ranges is highlighted in fig. 2b. E.g., in regime II_l with $Nu \sim Ra^{1/5}$ (for fixed Pr) the corresponding scaling exponent $1/5 - 1/4 = -1/20$ only becomes observable for very small $Pr \approx 10^{-3} - 10^{-4}$. At $Pr = 10^{-2}$ the roughly four decades of regime II_l (see figure 1) between regime I_l and IV_l , which both have a stronger Ra dependence of Nu , are not sufficient to reveal the scaling exponent. And at $Pr = 10^{-1}$ the roughly 2.5 decades of regime II_l are *nowhere* sufficient to lead to a local scaling exponent dNu/dRa smaller than $1/4$!

Similarly, for $Pr = 1$ only for very large $Ra \gtrsim 10^{15}$ pure scaling $Nu \sim Ra^{1/3}$ is revealed. For smaller Ra regimes I_u and I_l with $Nu \sim Ra^{1/4}$ strongly contribute, resulting in an

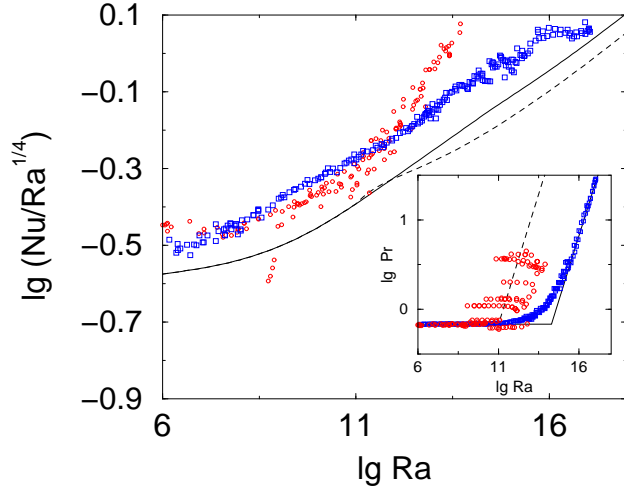


FIG. 3. $Nu(Ra, Pr(Ra))/Ra^{1/4}$ along the curve $Pr(Ra)$ given by the experimental restrictions of either the Niemela et al. experiment [6] (boxes in the inset and solid line in the main figure; the experimental data itself are shown as boxes) or the Chavanne et al. experiment [5] (circles in the inset and dashed line in the main figure; the experimental data itself are shown as circles). The simple parameterizations on which the curves in the main figures are based are also indicated.

effective local scaling exponent (increasing with Ra) in the range between 0.28 (“2/7”) and 0.31, just as observed in experiment [2, 3, 5, 6].

Direct comparison to experiment: Finally, let us point out that the present approach simplifies the comparison with experimental data: In experiment, it is hard to vary either Ra or Pr over many decades *and* at the same time to keep the other variable fixed. So most measurements are done along *curved* lines in the phase space figure 1, mixing the Ra and Pr dependences. Now eqs. (15) and (16) allow to calculate Nu and Re along such a curve $Pr(Ra)$ given by the experimental restrictions, which connect Ra and Pr . E.g., figure 3 shows $Nu(Ra, Pr(Ra))$ with $Pr(Ra)$ as resulting from the Niemela et al. [6] and the Chavanne et al. [5] experiments.

The present theory suggests that beyond $Ra \approx 10^{12}$ the Nusselt number in the Chavanne et al. experiment [5] should be *smaller* than in the Niemela et al. experiment [6], in contrast to what is found. This result is also in contrast to our former speculation of ref. [1], that the strong $Nu \sim Ra^{3/7}$ dependence of regime III_u , to which the Chavanne et al. data are closer, would account for their experimental findings. What we had overseen is that the larger Pr numbers of the Chavanne et al. experiment (for fixed Ra) and the $Nu \sim Pr^{-1/7}$ dependence of regime III_u overcompensates the strong Ra dependence of Nu for the Chavanne et al. data close to regime III_u .

This present theory cannot resolve the paradox between the Chavanne et al. and the Niemela et al. data. Possibly, different temperature boundary conditions have been applied. Possibly, Chavanne et al. have already observed the transition from a laminar to a turbulent kinetic BL (dotted line in the phase diagram fig. 1).

Acknowledgement: This research work was prompted by the experiments of G. Ahlers [9]. We thank him for sharing his results with us prior to publication and for various discussions.

-
- [1] S. Grossmann and D. Lohse, *J. Fluid. Mech.* **407**, 27 (2000).
 - [2] B. Castaing *et al.*, *J. Fluid Mech.* **204**, 1 (1989).
 - [3] E. D. Siggia, *Annu. Rev. Fluid Mech.* **26**, 137 (1994).
 - [4] S. Cioni, S. Ciliberto, and J. Sommeria, *J. Fluid Mech.* **335**, 111 (1997).
 - [5] X. Chavanne *et al.*, *Phys. Rev. Lett.* **79**, 3648 (1997).
 - [6] J. Niemela, L. Skrebek, K. R. Sreenivasan, and R. Donnelly, *Nature* **404**, 837 (2000).
 - [7] S. Ashkenazi and V. Steinberg, *Phys. Rev. Lett.* **83**, 3641 (1999).
 - [8] X. Xu, K. M. S. Bajaj, and G. Ahlers, *Phys. Rev. Lett.* **84**, 4357 (2000).
 - [9] G. Ahlers, 2000, seminar at the ITP-Workshop in Santa Barabara.
 - [10] R. Verzicco and R. Camussi, *J. Fluid Mech.* **383**, 55 (1999).
 - [11] J. Herring and R. Kerr, Preprint (2000).
 - [12] L. D. Landau and E. M. Lifshitz, *Fluid Mechanics* (Pergamon Press, Oxford, 1987).
 - [13] B. I. Shraiman and E. D. Siggia, *Phys. Rev. A* **42**, 3650 (1990).
 - [14] G. O. Roberts, *Geophys. Astrophys. Fluid Dyn.* **12**, 235 (1979).
 - [15] P. Constantin and C. Doering, *J. Stat. Phys.* **94**, 159 (1999).